SUPPORTING INFORMATION

Crystalline Microporous Small-molecule Semiconductors Based on Porphyrin for High-performance Chemiresistive Gas Sensing

Wei-Hua Deng,†[abc] Liang He,†[abc] Er-Xia Chen,[ac] Guan-E Wang,[a] Xiao-Liang Ye,[a] Zhi-Hua Fu,[a] Qipu Lin*[abc] and Gang Xu*[abc]

Table S1. Crystallographic data of **2**

Compound name	**2**
Empirical formula	$C_{96}H_{57}N_8O_{16}$, 2(H_4N), 2(C_2H_3N)
Formula weight	1948.91
Temperature/K	293
Crystal system	monoclinic
Space group	$P2_1/n$
a/Å	22.6949
b/Å	9.6108
c/Å	23.3758
α/°	90
β/°	97.186
γ/°	90
Volume/Å^3	7905.5(3)
Z	2
ρ_{calc}/g cm^{-3}	1.280
μ/mm^{-1}	0.402
F(000)	1766
Radiation	GaK α (λ = 1.34050)
2ϑ range for data collection/°	4.448~105.864
Collected reflections	38175
Independent reflections	8918 [R_{int} = 0.0432, R_{sigma} = 0.0360]
Goodness-of-fit on F^2	1.075
Final R indexes [I>=2σ(I)]	[a]R_1 = 0.0477, [b]wR_2 = 0.1313
Final R indexes [all data]	[a]R_1 = 0.0605, [b]wR_2 = 0.1393
CCDC No.	2127390

[a] $R_1 = \sum||F_o| - |F_c||/\sum|F_o|$; [b] $wR_2 = [\sum w(F_o^2 - F_c^2)^2/\sum w(F_o^2)^2]^{1/2}$.

Powder X-Ray diffraction (PXRD)

PXRD patterns were collected for polycrystalline samples using a Rigaku Dmax 2500 X-ray diffractometer using copper radiation (Cu K_α, λ = 1.5418 Å). Profiles were collected at rt in the angular range 3° < 2ϑ < 45° with a step size of 0.02. Molecular modeling was carried out using Reflex Plus, a module implemented in Materials Studio (version 4.4) by Accelrys Inc. The initial structure of **1** was constructed piecewise starting with a triclinic space group *P*-1. The Pseudo-Voigt function was used for whole profile fitting and Berrar-Baldinozzi function was used for asymmetry correction during the refinement processes. The predicted structure was validated with Rietveld refinements against the observed PXRD patterns.

Table S2. Refinement parameters of **1**

Compound name	**1**
Refined composition	$C_{48}H_{30}N_4O_8$
Formula weight	790.76
Crystal system	triclinic
Space group	*P*-1
a/Å	8.1865
b/Å	16.210
c/Å	19.978
α/°	74.981
β/°	80.473
γ/°	84.737
Volume/Å^3	2521.9
Z	2
ρ_{calc}/g cm^{-3}	1.041
2ϑ range for data collection/°	3~45
R_p (%) [Rietveld]	6.84
R_{wp} (%) [Rietveld]	8.63

Table S3. Atomic coordinates of **1**

Atom	x	y	z
O1	0.21027	0.13501	0.89336
O2	0.30200	0.04124	0.82937
H2	0.32061	0.04035	0.78795
O3	-0.06419	0.23397	0.13235
O4	0.17990	0.16876	0.15425
H4	0.16068	0.14150	0.12736
O5	0.24418	1.00708	-0.00703
H5	0.29629	1.04611	-0.03426
O6	0.12329	0.06026	1.08988
O7	0.30654	0.94722	0.74702
O8	0.55313	0.97604	0.68939
H8	0.62721	0.94969	0.6692
N1	0.28234	0.69579	0.42071
N2	0.29317	0.55402	0.54159
H2A	0.26447	0.56569	0.50052
N3	0.20430	0.43850	0.46015
N4	0.23277	0.59131	0.33549
H4A	0.23221	0.58789	0.37921
C1	0.26269	0.11381	0.83398
C2	0.16265	0.26580	0.77392
H2B	0.11080	0.27318	0.81720
C3	0.24444	0.18810	0.76898
C4	0.32195	0.17707	0.70429
H4B	0.37667	0.12509	0.70099
C5	0.31766	0.24374	0.64455
H5A	0.36952	0.23636	0.60127
C6	0.23587	0.32143	0.64949
C7	0.15836	0.33246	0.71417
H7	0.10364	0.38445	0.71748
C8	0.06046	0.22245	0.16225
C9	0.08994	0.27904	0.20838
C10	0.21704	0.25558	0.24898
H10	0.28422	0.20661	0.24673
C11	0.24373	0.30530	0.29296
H11	0.32876	0.28960	0.32012
C12	0.14331	0.37850	0.29633
C13	0.01622	0.40196	0.25573
H13	-0.05097	0.45093	0.25799
C14	-0.01047	0.35224	0.21176
H14	-0.09551	0.36794	0.18459
C15	0.42574	0.93826	0.70169
C16	0.42062	0.87003	0.65899

C17	0.29602	0.81211	0.68286
H17	0.22708	0.81128	0.72497
C18	0.27447	0.75542	0.64378
H18	0.19111	0.71666	0.65974
C19	0.37752	0.75666	0.58084
C20	0.50211	0.81459	0.55698
H20	0.57106	0.81542	0.51487
C21	0.52367	0.87127	0.59605
H21	0.60703	0.91003	0.58009
C22	0.20276	1.02460	0.05085
C23	0.22485	0.95634	0.11848
C24	0.11177	0.95013	0.17947
H24	0.02712	0.99211	0.1818
C25	0.12520	0.88119	0.23690
H25	0.04954	0.87704	0.27771
C26	0.25172	0.81844	0.23333
C27	0.36480	0.82465	0.17234
C28	0.35137	0.89359	0.11492
H28	0.42703	0.89774	0.07411
C29	0.16857	0.43471	0.34025
C30	0.16304	0.40055	0.41259
C31	0.10235	0.31460	0.45112
H31	0.06200	0.27459	0.43285
C32	0.11956	0.30769	0.52031
H32	0.08654	0.26251	0.55826
C33	0.19750	0.38269	0.52322
C34	0.23809	0.39554	0.58733
C35	0.29642	0.47424	0.58684
C36	0.36665	0.48218	0.64592
H36	0.39084	0.43836	0.68392
C37	0.39104	0.56818	0.63488
H37	0.43329	0.59336	0.66481
C38	0.34124	0.61017	0.57120
C39	0.34095	0.69615	0.53850
C40	0.30317	0.73656	0.46889
C41	0.29867	0.83074	0.44015
H41	0.30704	0.87426	0.46174
C42	0.27848	0.83496	0.37217
H42	0.27505	0.88705	0.3390
C43	0.26295	0.75590	0.35449
C44	0.26025	0.74365	0.29300
C45	0.24823	0.66076	0.28341
C46	0.25287	0.64230	0.21683
H46	0.26831	0.68027	0.17282
C47	0.23056	0.56005	0.23151

H47	0.22415	0.52924	0.19879
C48	0.21765	0.52514	0.30530

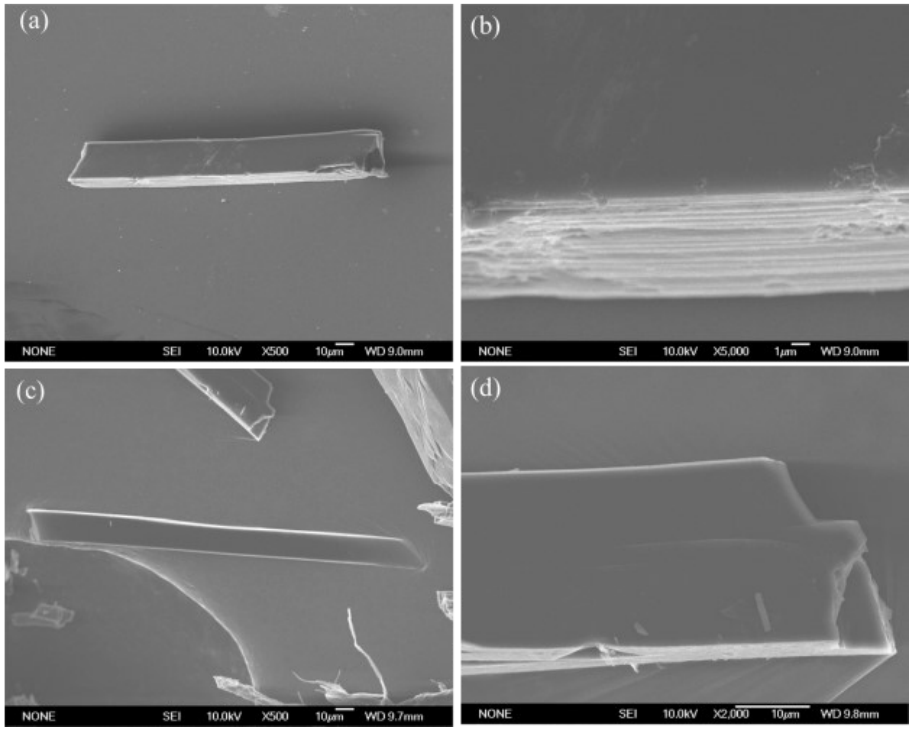

Figure S1. (a, b) SEM images of compound **1**; (c, d) SEM images of compound **2**.

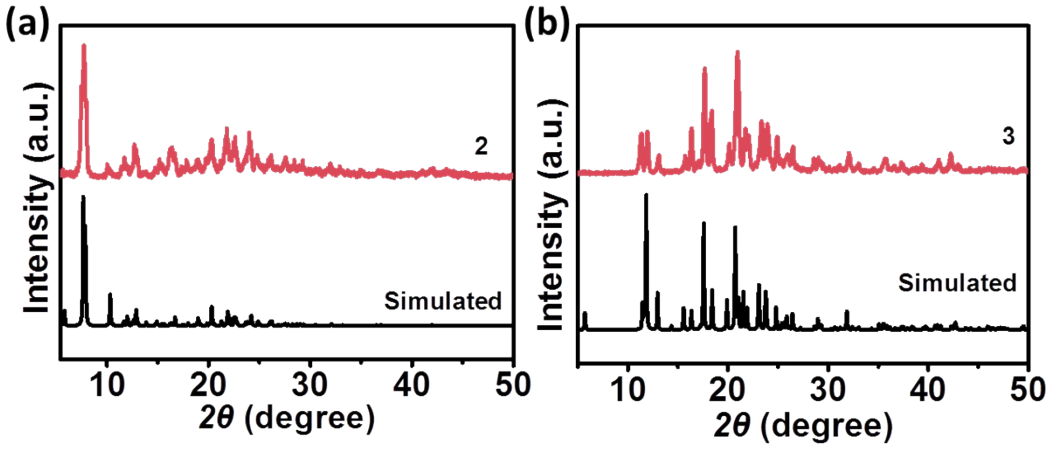

Figure S2. PXRD patterns of (a) **2** and (b) **3**.

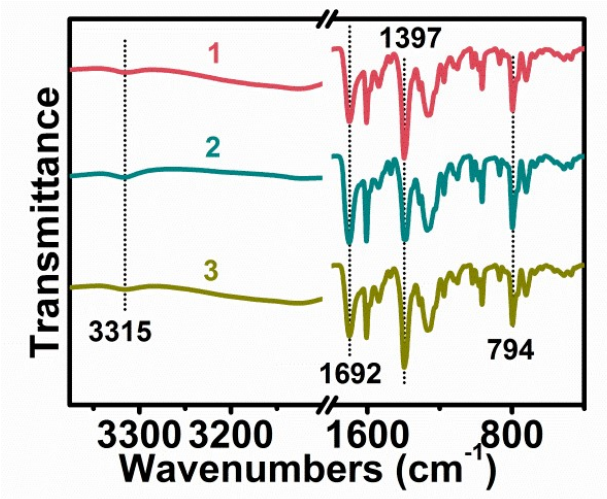

Figure S3. FT-IR spectra of **1**, **2** and **3**. The as-synthesized samples **1**, **2** and **3** have similar spectra, where the band at 3330~3300 cm^{-1} was assigned to the stretching vibration bond of -NH, the peak near 1390 cm^{-1} for the characteristic vibration of $-C_{\alpha}N$, $-C_{\alpha}C_{\beta}$ and the bands at 1750~1620 cm^{-1} were due to -C = O in carboxylic acid.[1]

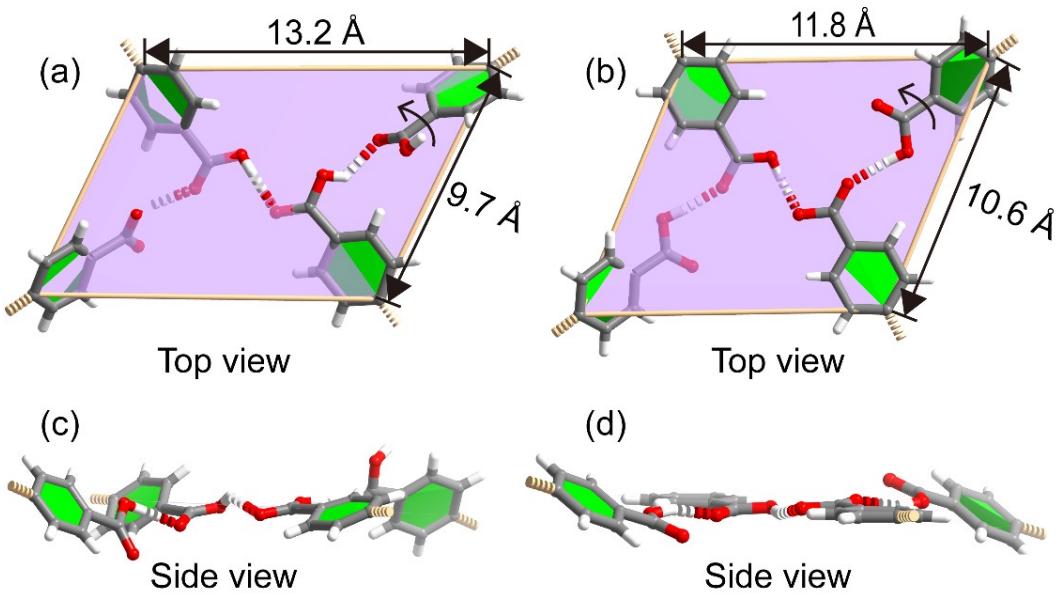

Figure S4. (a) The hydrogen-bonding node A for **1** (a and c) and node B for **2** (b and d).

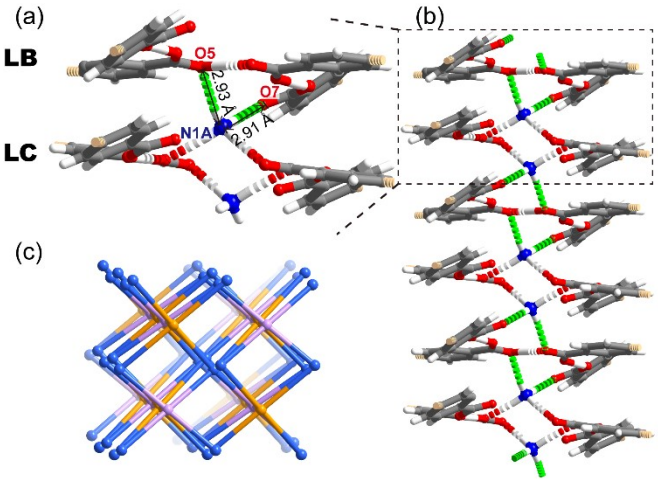

Figure S5. Hydrogen bonding chain built of LB and LC nodes for **2**.

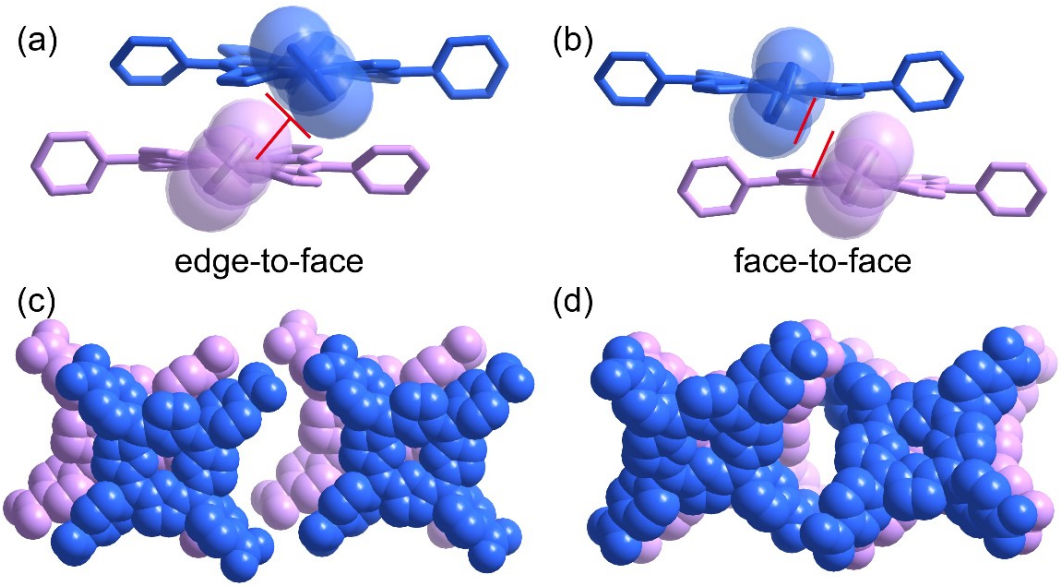

Figure S6. The π–π interaction modes between adjacent benzene rings for **1** (a) and **2** (b), and the relative positions of the two neighbouring porphyrins for **1** (c) and **2** (d).

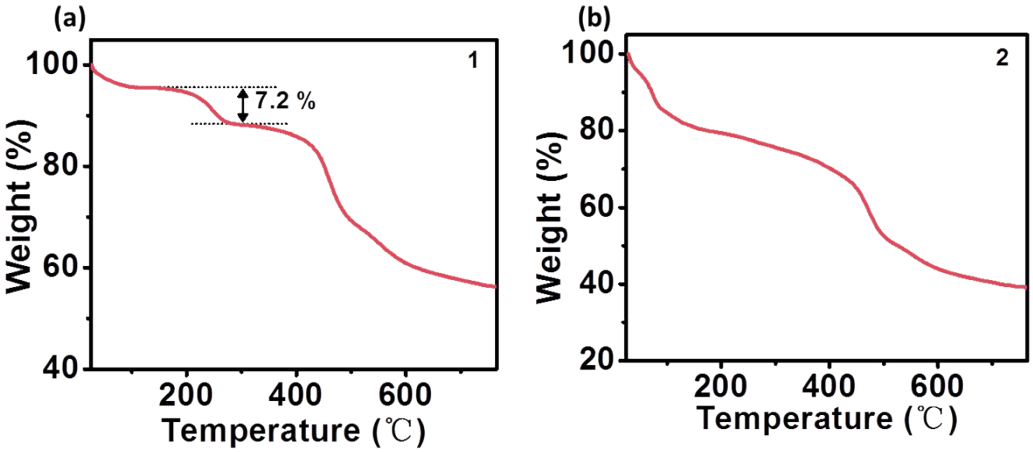

Figure S7. TGA curves of (a) **1** and (b) **2**.

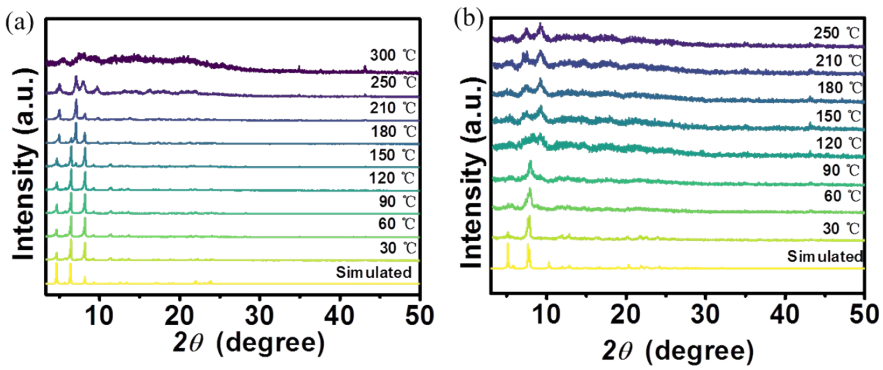

Figure S8. Various temperature PXRD patterns of (a) **1** and (b) **2**.

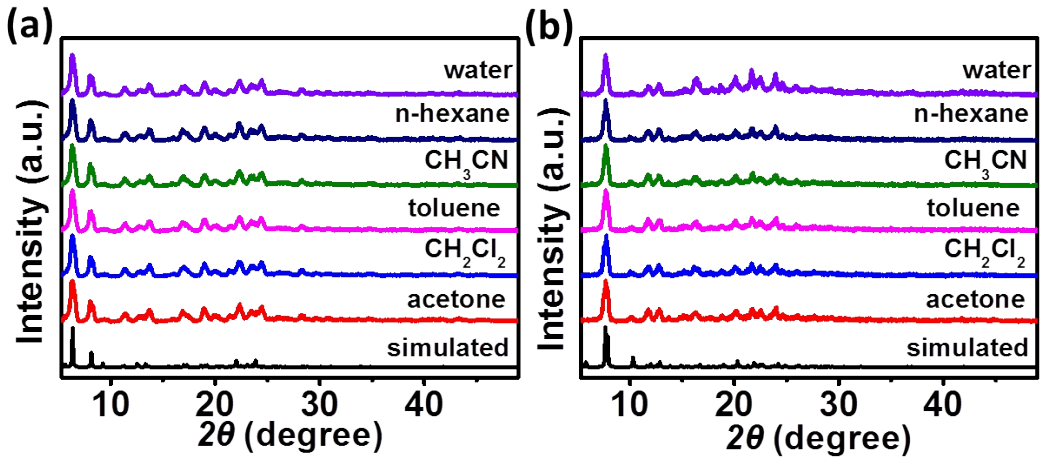

Figure S9. PXRD patterns of (a) **1** and (b) **2** samples after soaking in water or organic solvents (acetone, dichloromethane (CH_2Cl_2), toluene, acetonitrile (CH_3CN), and *n*-hexane) for at least 12 h.

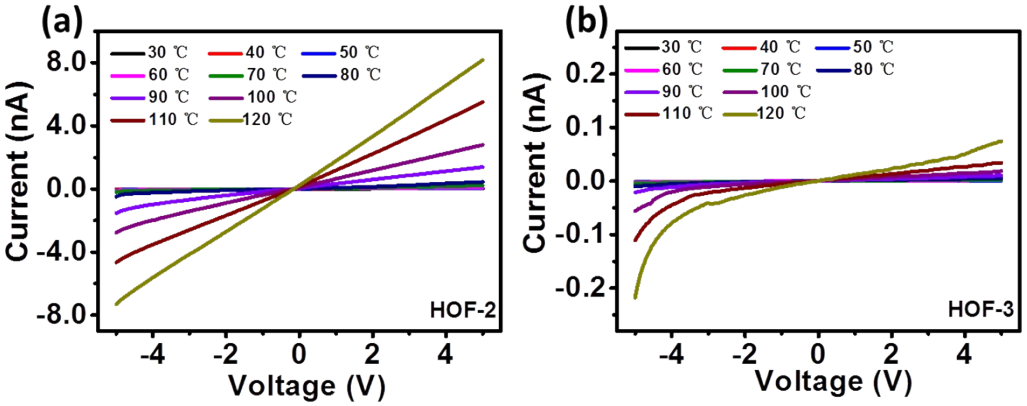

Figure S10. Temperature-dependent I–V curves of (a) **2** and (b) **3**.

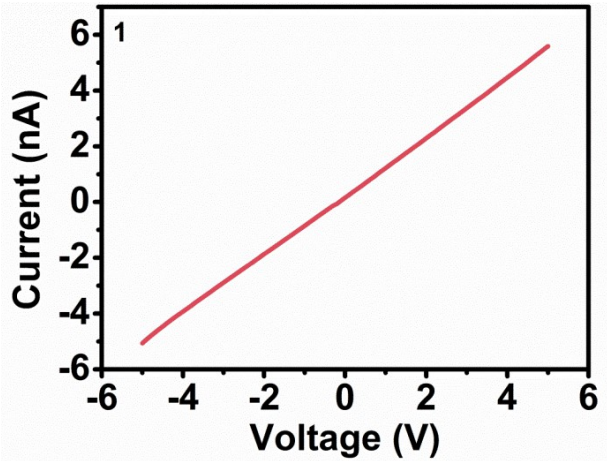

Figure S11. I–V curve of **1** at rt and under visible light irradiation

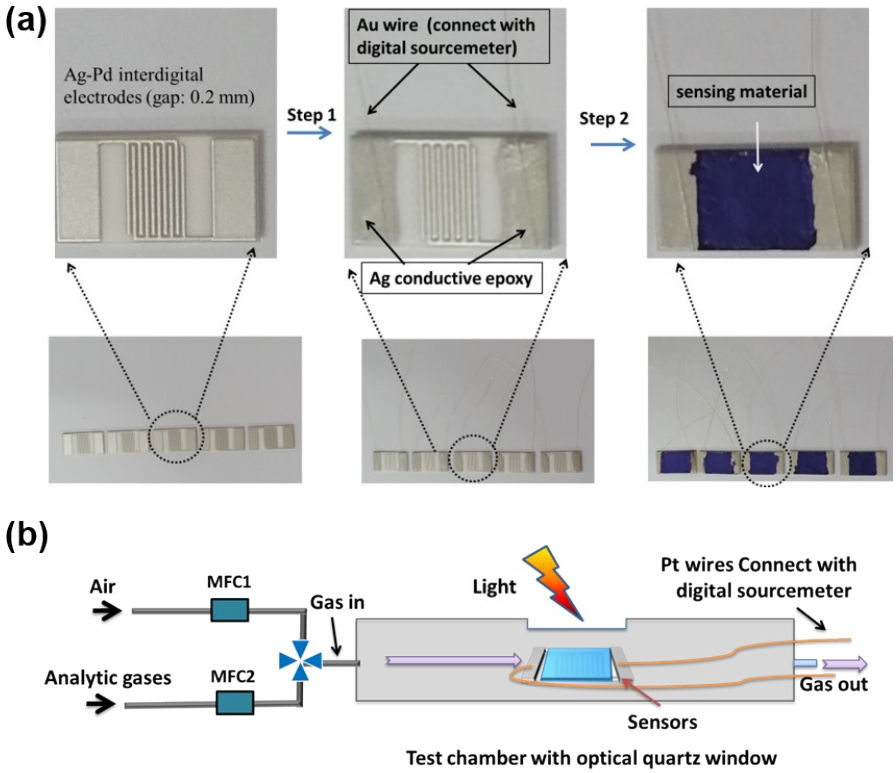

Figure S12. (a) Photographs of sensor devices in this manuscript. (b) Schematic illustration of the gas-detection equipment at rt and under visible light irradiation.

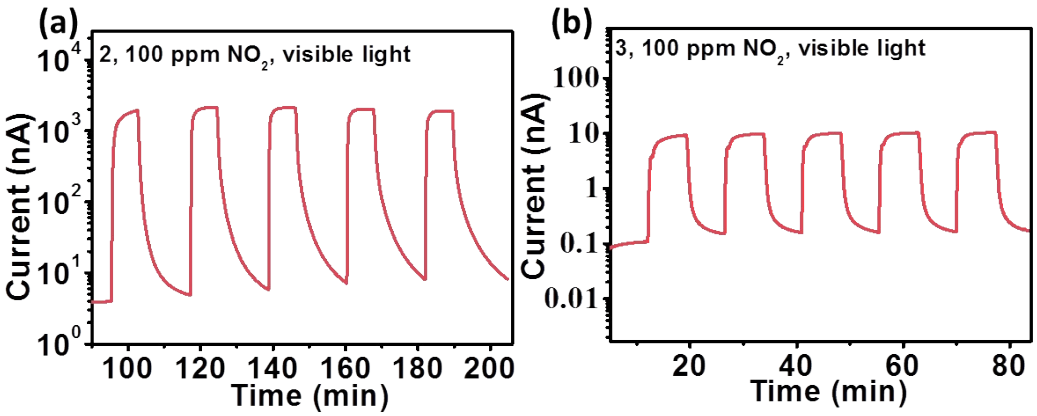

Figure S13. Dynamic response–recovery successive cycling curves for (a) **2** and (b) **3** toward 100 ppm NO_2 at rt and under visible light irradiation.

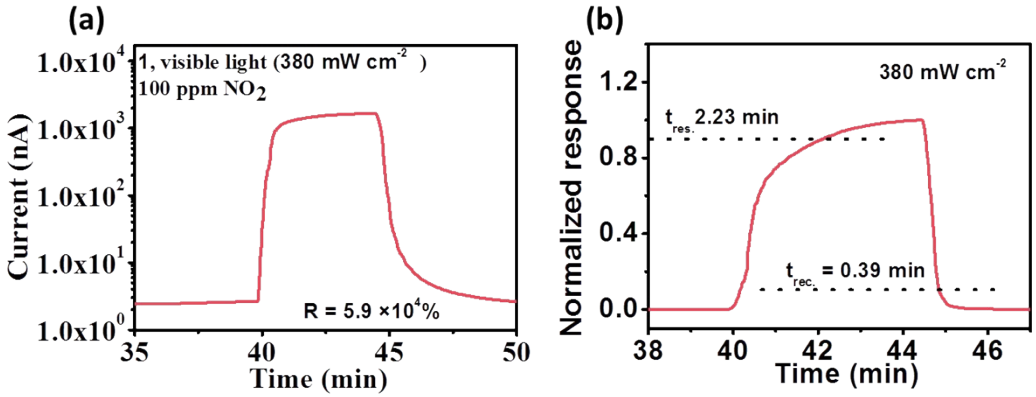

Figure S14. (a) Dynamic response–recovery curves and (b) response and recovery time for **1** toward 100 ppm NO_2 at rt and under visible light irradiation (380 mW cm^{-2}).

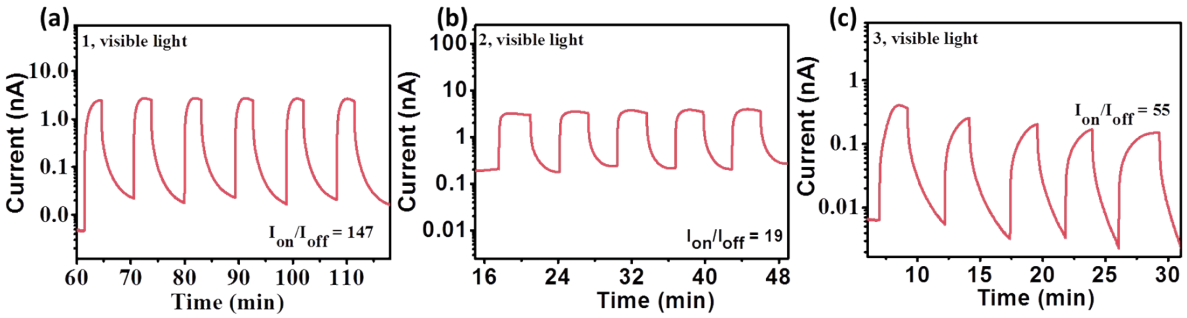

Figure S15. Transient photocurrent responses of (a) **1**, (b) **2** and (c) **3** at rt and under visible light irradiation.

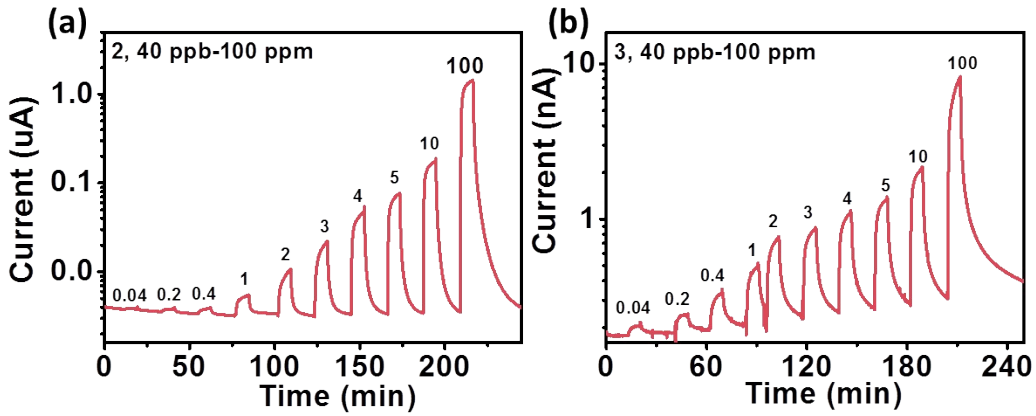

Figure S16. Dynamic response–recovery curves of NO_2 sensing properties of (a) **2** and (b) **3** sensor in a concentration ranging of 0.04-100 ppm under visible light irradiation at rt.

Table S4. NO_2 sensing performances of different sensor devices at rt.

Sensing materials	tres/trec (min)	Response (R_{gas}/R_{air}-1)%	Concentration (ppm)	LOD (ppb)	Ref.
1	**2.5/0.6**	**1.7×10^5**	**100**	**20(exp.)**	**This work**
3D graphene Flowers	33/0.03	1411	10	100(exp.)	[2]
3D graphene	8.3/50	74	10	-[k]	[3]
Graphene	~[j]10/10	27	5	-	[4]
Graphene/MoS_2	10/10	12	0.5	50	[5]
Graphene/CeO_2	0.31/4.1	5	10	5000	[6]
RGO	3.3-5/5	4	100	-	[7]
RGO	>5/>10	150	100	2000	[8]
RGO	15/20	815	100	-	[9]
RGO@Cu_2O	5/8	67	2	400	[10]
RGO/PET	3/5	6	10	500(exp.)[n]	[11]
sulfonated RGO	~ 8.3 /41	~ 640	20	2000	[12]
RGO/MoS_2	5/7.5	~ 40	10	53	[13]
3D FRGOH[a]	7/13	8	10	57	[14]
3D S-RGOH[b]	~6.5/0.18	23	4	200(exp.)	[15]
RGO–IDTO[c]	>10/ > 16	1100	100	300(exp.)	[16]
Ag-S-RGO	0.2/0.33	90	100	500(exp.)	[17]
RGO/ SnO_2	1.1/incomplete recovery	120	10	1000 (exp.)	[18]
CNT[d]	3/10	84	100	250(exp.)	[19]
CNT	10/10	90	10	44	[20]
CNTs/Au	-[k]	10	1	100	[21]
CNTs/SnO_2	⍰4.5/⍰3.5	40	25	-	[22]
SnO_2	1/12	~80	10	2000(exp.)	[23]
SnO-SnO_2	0.95/5	500	10	100	[24]
amine-terminated SnO_2	1.8/1.25	2100	0.4	250 (exp.)	[25]
ZnO	3.7/2	410	20	-	[26]
ZnO	15/48	120	20	-	[27]
ZnO1-x	13.7/15	259	1	-	[28]
$SnO_{1-\alpha}$@$ZnO_{1-\beta}$@$SnO_{2-\gamma}$	17.6/23.4	236	1	-	[29]
ZnO /RGO	1.25/2.2	119	1	-	[30]
ZnO-Ag	2.5/2.16	110	1	-	[31]
CdS/ZnO	0.45/3.8	337	1	5(exp.)	[32]
SnO_2/ZnO	1.5/3.7	619	5	1000(exp.)	[33]
ZnO/SnO_2	7/8	1×10^5	0.5	200(exp.)	[34]
ZnO/PbS	3/4	500	10	-	[35]
MoS_2/SnO_2	6.8/1.2	28	10	500(exp.)	[36]
P_3HT[f] /ZnO	15/45	90	10	-	[37]
Au/ZnO	25/⍰40	60	5	-	[38]
$TiO_{2-x}N_x$	~ 6/6	~ 14	10	-	[39]
Polypyrrole /WO_3	10/~91	16	10	5000(exp.)	[40]
RGO/WO_3	9/18	769	5	-	[41]
DBSA doped PPy–WO_3	4.8/99.8	72	100	-	[42]

Polypyrrole–NiO	2.08/8.3	8	10	10000(exp.)	[43]
In_2O_3/RGO	4/24	725	30	-	[44]
In_2O_3	10/15	61800	0.5	50 (exp.)	[45]
MoS_2	8/25	60	100	-	[46]
MoS_2	11.3/5.3	11	10	1000	[47]
MoS_2 -Pt	>30/30	18	5	-	[48]
CdS	0.73/1.88	89	5	100	[49]
WS_2@MTCNF[e]	3.73/10	28	4	10	[50]
Ag/WS_2	~5/10	58	25	1000(exp.)	[51]
PbS CQDs[g]	0.2/0.61	2170	50	500 (exp.)	[52]
Si	1.38/0.3($t_{50\%}$, microheater)	80	100	1000	[53]
Te	1.4/13 ($t_{50\%}$)[m]	62	10	100(exp.)	[54]
Black Phosphorus	0.08/10	100	100	100(exp.)	[55]
Phosphorene	~10/10	9000	1	~ 20(exp.)	[56]
polythiophene	4.95/9.75	9	10	10000(exp.)	[57]
Electrospun polyaniline	1/-	80	1	~50	[58]
VOPc/F_{16}CuPc[h]	10/12	700	5	500(exp.)	[59]
PTCDI-Ph/p-6P[i]	~ 30/60	670	30	5000(exp.)	[60]
$CH_3NH_3PbI_{3x}(SCN)_x$	3.7/6	300	5	200	[61]
CuTAP(t-Bu)$_4$[p]	4.5/9	500	50	-	[62]
metal-thiourea complex	2.9/9.2	19000	10	-	[63]
polythiophene	3.7/26.7	33	100	-	[64]
Ag(SPh–NH_2)	1/2.3	852	10	100	[65]
rGO/P NFs	4/10	250	5	150(exp.)	[66]
graphene	5/10	15	5	5000 (exp.)	[67]
graphene nanomesh	15/20	12	10	1000 (exp.)	[68]
rGO/Au	7/28	25	20	1000 (exp.)	[69]
rGO/Au	5/>11	50	8	200 (exp.)	[70]
CuPc	1.3/1.6	17	0.5	50 (exp.)	[71]
$MnPS_3$	1.6/2.6	9530	35	100 (exp.)	[72]
MoS_2	1/> 10	200	1	120 (exp.)	[73]
SnO_2 /MCN[O]	7/12	1.1×10^5	0.1	100 (exp.)	[74]
g–C_3N_4/SnS_2	-/2.76	1750	6	125 (exp.)	[75]
SnS_2/MoS_2	0.03/0.5	2490	100	50 (exp.)	[76]
Black Phosphorus	8.3/5	30	0.04	5 (exp.)	[77]
MoS_2/GR	0.36/0.58	30	100	100000(exp)	[78]
UPC-H4a	0.28/0.26	43	2	40(exp)	[79]
Si-doped graphene	2.1/6.3	21.5	50	18(exp)	[80]
Pd-SnO_2-rGO	0.21/1.75	292	1	50(exp)	[81]
B-RGOH	-/1.58	25.3	0.8	20(exp)	[82]
N-RGOH	-/0.16	13	0.8	50(exp)	[82]
Metal phthalocyanine/ graphene	1.67/1.67	1480	50	50(exp)	[83]
cobalt phthalocyanine	1.67/1.67	512	50	50(exp)	[84]
GaN/TiO_2	2.3/2.6	32	500	1(exp)	[85]
MoS_2	0.26/1.08	670	0.4	20(exp)	[86]

VO-rich ZnO nanowires	0.51/2.4	708	1	20(exp)	[87]
MoS_2/ZnO	0.33/0.33	607	1	50(exp)	[88]
ZnO quantum dots	2.5/1	650	1	50(exp)	[89]
TiO_2/graphene	0.5/1.5	330	1.75	70(exp)	[90]
SnO_2	0.11/0.42	3400	10	100(exp)	[91]
Pd-SnO_2-RGO	0.21/1.75	292	1	50(exp)	[92]
Pt-In_2O_3	-/5.96	2290	1	10(exp)	[93]
Pd-In_2O_3	4.5/4.7	950	0.5	100(exp)	[94]
$MoTe_2$	/2.7	7000	2	20(exp)	[95]
ZnO	2.9/6.2	100	0.15	25(exp)	[96]

a: 3D FRGOH (3D chemically functionalized reduced graphene oxide hydrogel); b: 3D S-RGOH (3D sulfonated RGO hydrogel); c: RGO–IDTO (Indium-doped SnO_2–graphene), d: CNT (single walled carbon nanotube); e: WS_2@MTCNFs (WS_2 edge functionalized carbon nanofibers); f: P_3HT (poly(3-hexylthiophene)); g: PbS CQDs (PbS Colloidal Quantum Dots); h: VOPc/ $F_{16}CuPc$ (vanadyl phthalocyanine/ copper hexadecafluoro-phthalocyanine); i: PTCDI-Ph/p-6P (N,N'-diphenyl perylene tetracarboxylic diimide / para-hexaphenyl) ; j: "~" means estimated value of figure obtained; k: "-" means cannot extracted the information from the article; m: the response time $t_{50\%}$ is defined as the time to achieve 50% of its steady resistance in the response process, and the recovery time $t_{50\%}$ is defined as the time to reach 50% of its original resistance in the signal recovery process; n: "exp." means experimental detection limits; o: MCN (multiwalled carbon nanotubes). p: CuTAP(t-Bu)$_4$ (tetra-(tert-butyl)-5,10,15,20-tetraazaporphyrin copper)

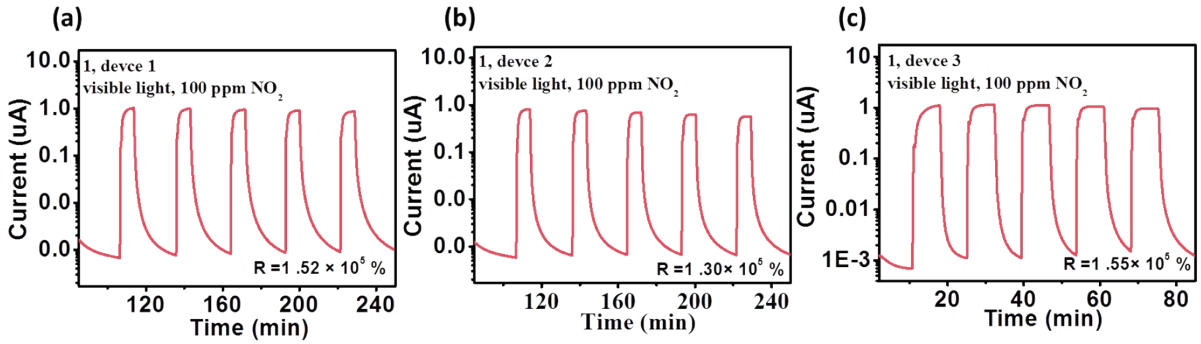

Figure S17. Dynamic response-recovery curves of three different **1** sensor toward 100 ppm NO_2 at rt and under visible light irradiation.

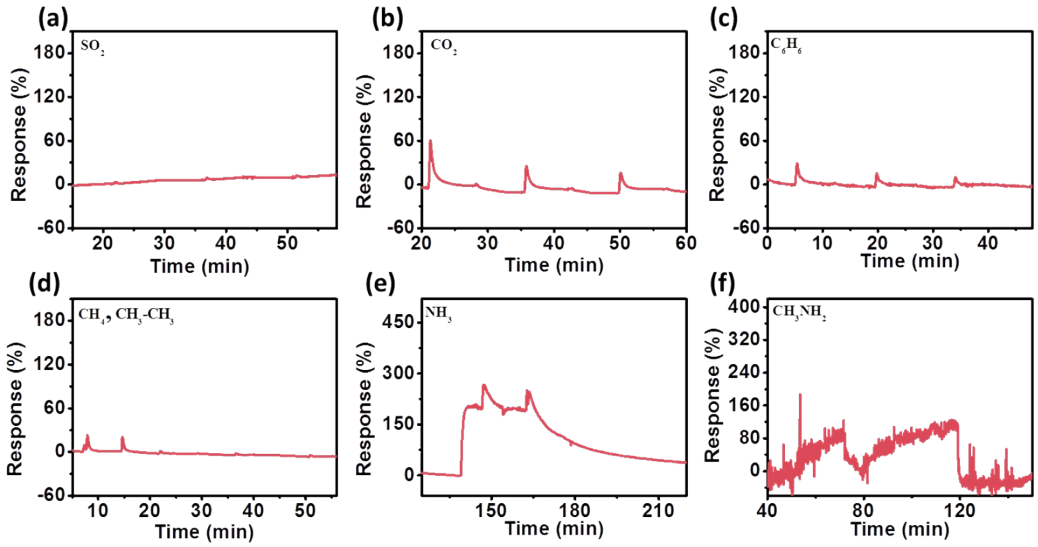

Figure S18. Dynamic response curves of **1** sensor against 100 ppm of typical interference gases under visible light at rt. (a) SO_2, (b) CO_2, (c) C_6H_6, (d) CH_4 and CH_3-CH_3, (e) NH_3, (f) CH_3NH_2.

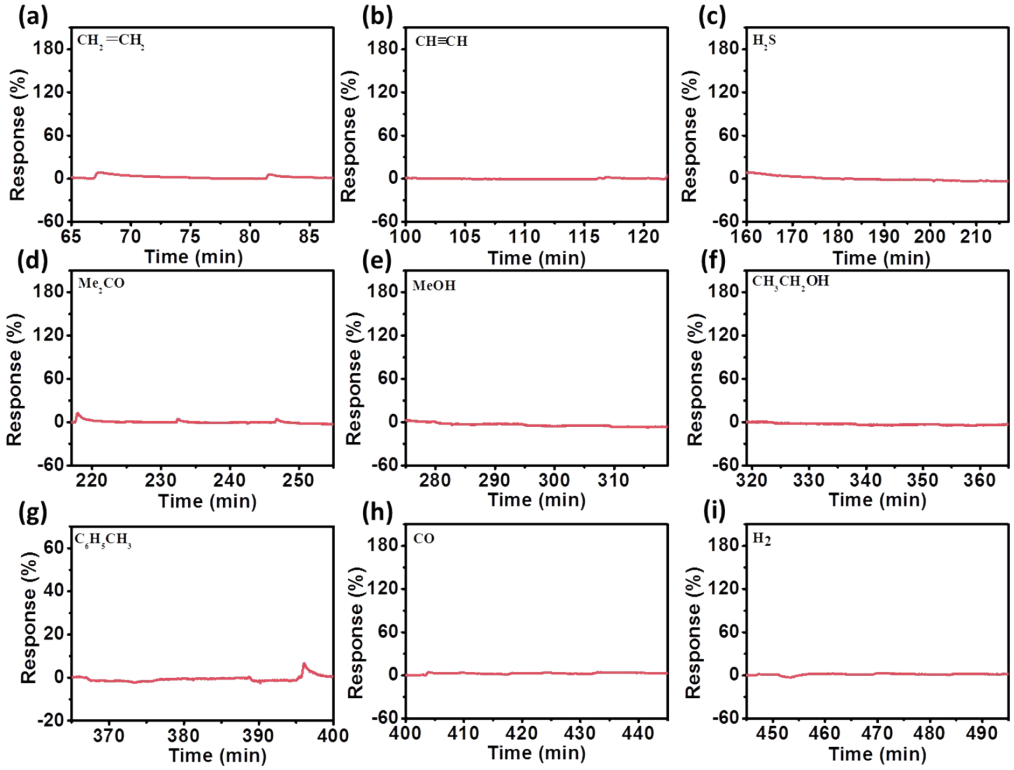

Figure S19. Dynamic response curves of **1** sensor against 100 ppm of typical interference gases under visible light at rt. (a) CH_2=CH_2, (b) CH≡CH, (c) H_2S, (d) Me_2CO (e) MeOH, (f) CH_3CH_2OH, (g) $C_6H_5CH_3$, (h) CO, (i) H_2.

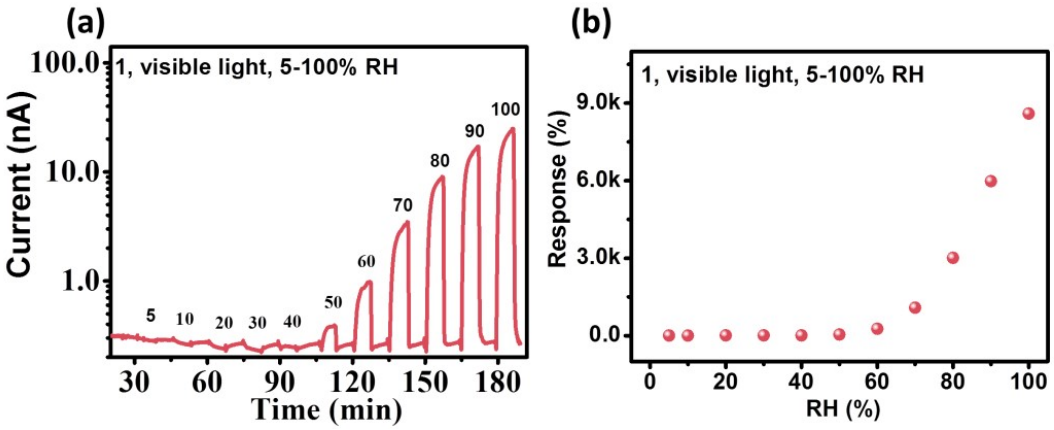

Figure S20. Sensing results of **1** toward H_2O at rt and under visible light irradiation, (a) real-time dynamic response-recovery curve in the concentration range of 5%~100% RH, (b) response versus [RH%] graph.

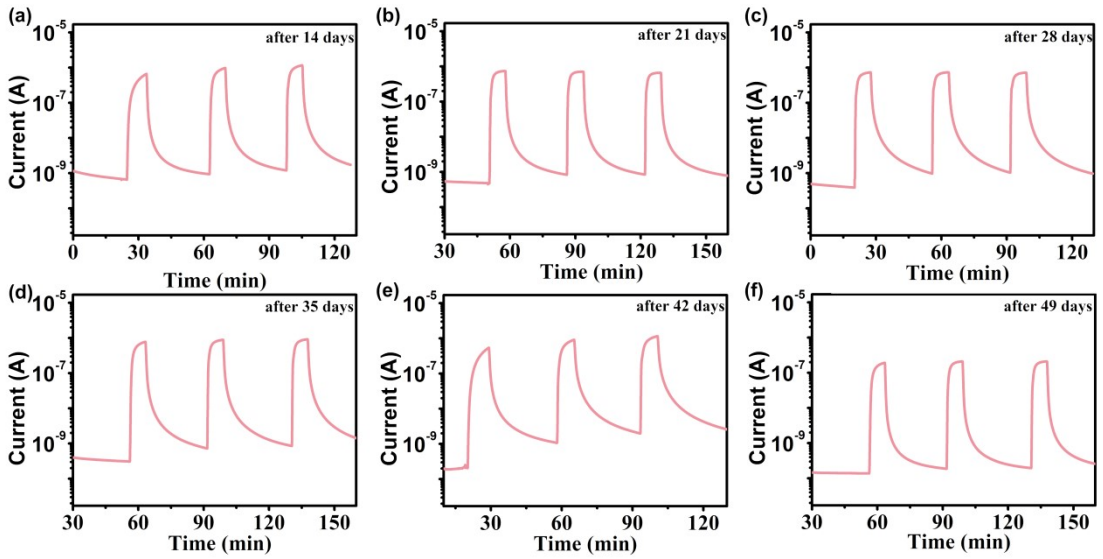

Figure S21. (a-f) the response-recovery curves of **1** towards NO2 in 7 weeks.

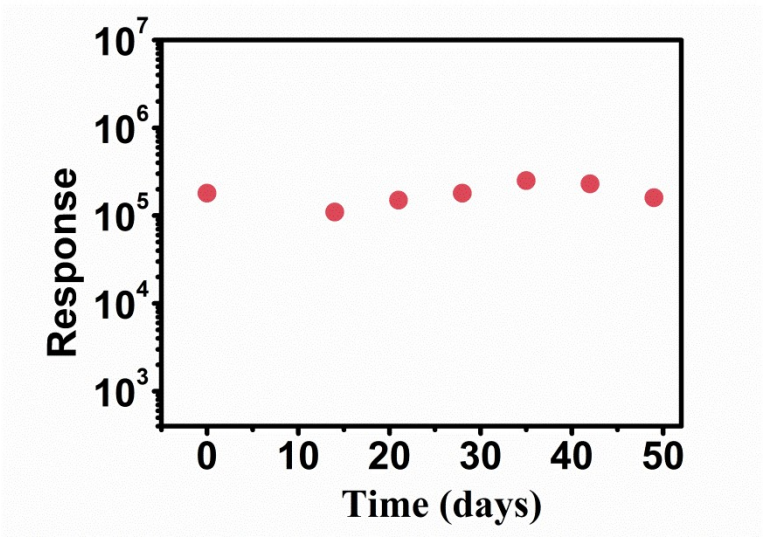

Figure S22. The long-term stability of **1** for NO_2 detection.

$$2NO_2 + O^{2-} \rightarrow NO_3^- + NO_2^- \quad (1)$$

$$NO_2 + e^- \leftrightarrow NO_2^- \quad (2)$$

$$NO_2 + O_2^- + 2e^- \leftrightarrow NO_2^- + 2O^- \quad (3)$$

$$NO_2 + 2e^- \leftrightarrow NO_3^- + NO^- \quad (4)$$

References

[1] Hayashi K., Nakamura M., Miki H., Ozaki S., Abe M., Matsumoto T., Ishimura K., *Adv. Funct. Mater.* **2012**, *22*, 3539-3546.
[2] Wu J., Feng S., Wei X., Shen J., Lu W., Shi H., Tao K., Lu S., Sun T., Yu L., Du C., Miao J., Norford L. K., *Adv. Funct. Mater.* **2016**, *26*, 7462-7469.
[3] Chen Z., Wang J., Umar A., Wang Y., Li H., Zhou G., *ACS Appl. Mater. Inter.* **2017**, *9*, 11819-11827.
[4] Fowler J. D., Allen M. J., Tung V. C., Yang Y., Kaner R. B., Weiller B. H., *ACS Nano* **2009**, *3*, 301-306.
[5] Long H., Harley-Trochimczyk A., Thang P., Tang Z., Shi T., Zettl A., Carraro C., Worsley M. A., Maboudian R., *Adv. Funct. Mater.* **2016**, *26*, 5158-5165.
[6] Yang Y., Tian C., Sun L., Lu R., Zhou W., Shi K., Kan K., Wang J., Fu H., *J. Mater. Chem. A.* **2013**, *1*, 12742-12749.
[7] Han T. H., Huang Y.-K., Tan A. T. L., Dravid V. P., Huang J., *J. Am. Chem. Soc.* **2011**, *133*, 15264-15267.
[8] Lu G., Ocola L. E., Chen J., *Nanotechnology* **2009**, *20*, 445502-445511.
[9] Lu G., Park S., Yu K., Ruoff R. S., Ocola L. E., Rosenmann D., Chen J., *ACS Nano* **2011**, *5*, 1154-1164.
[10] Deng S., Tjoa V., Fan H. M., Tan H. R., Sayle D. C., Olivo M., Mhaisalkar S., Wei J., Sow C. H., *J. Am. Chem. Soc.* **2012**, *134*, 4905-4917.
[11] Dua V., Surwade S. P., Ammu S., Agnihotra S. R., Jain S., Roberts K. E., Park S., Ruoff R. S., Manohar S. K., *Angew. Chem. Int. Ed.* **2010**, *49*, 2154-2157.
[12] Yuan W., Liu A., Huang L., Li C., Shi G., *Adv. Mater.* **2013**, *25*, 766-771.
[13] Niu Y., Wang R., Jiao W., Ding G., Hao L., Yang F., He X., *Carbon* **2015**, *95*, 34-41.
[14] Wu J., Tao K., Zhang J., Guo Y., Miao J., Norford L. K., *J. Mater. Chem. A.* **2016**, *4*, 8130-8140.
[15] Wu J., Tao K., Guo Y., Li Z., Wang X., Luo Z., Feng S., Du C., Chen D., Miao J., Norford L. K., *Adv. Sci.* **2017**, *4*, 1600319-1600328.
[16] Cui S., Wen Z., Mattson E. C., Mao S., Chang J., Weinert M., Hirschmugl C. J., Gajdardziska-Josifovska M., Chen J., *J. Mater. Chem. A.* **2013**, *1*, 4462-4467.
[17] Huang L., Wang Z., Zhang J., Pu J., Lin Y., Xu S., Shen L., Chen Q., Shi W., *ACS Appl. Mater. Inter.* **2014**, *6*, 7426-7433.
[18] Mao S., Cui S., Lu G., Yu K., Wen Z., Chen J., *J. Mater. Chem.* **2012**, *22*, 11009-11013.
[19] Ammu S., Dua V., Agnihotra S. R., Surwade S. P., Phulgirkar A., Patel S., Manohar S. K., *J. Am. Chem. Soc.* **2012**, *134*, 4553-4556.
[20] Li J., Lu Y. J., Ye Q., Cinke M., Han J., Meyyappan M., *Nano Lett.* **2003**, *3*, 929-933.
[21] Zanolli Z., Leghrib R., Felten A., Pireaux J.-J., Llobet E., Charlier J.-C., *ACS Nano* **2011**, *5*, 4592-4599.
[22] Lu G., Ocola L. E., Chen J., *Adv. Mater.* **2009**, *21*, 2487-2491.
[23] Law M., Kind H., Messer B., Kim F., Yang P. D., *Angew. Chem. Int. Ed.* **2002**, *41*, 2405-2408.
[24] Yu H., Yang T., Wang Z., Li Z., Zhao Q., Zhang M., *Sensor. Actuat. B-Chem.* **2018**, *258*, 517-526.
[25] Hoffmann M. W. G., Daniel Prades J., Mayrhofer L., Hernandez-Ramirez F., Jaervi T. T., Moseler M., Waag A., Shen H., *Adv. Funct. Mater.* **2014**, *24*, 595-602.
[26] Meng L., Xu Q., Sun Z., Li G., Bai S., Wang Z., Qin Y., *Mater. Lett.* **2018**, *212*, 296-298.
[27] Fan S.-W., Srivastava A. K., Dravid V. P., *Sensor. and Actuat. B-Chem.* **2010**, *144*, 159-163.
[28] Zhang C., Geng X., Liao H., Li C.-J., Debliquy M., *Sensor. Actuat. B-Chem.* **2017**, *242*, 102-111.
[29] Geng X., Zhang C., Luo Y., Liao H., Debliquy M., *Ceram. Int.* **2017**, *43*, 5990-5998.
[30] Xia Y., Wang J., Xu J.-L., Li X., Xie D., Xiang L., Komarneni S., *ACS Appl. Mater. Inter.* **2016**, *8*, 35454-35463.
[31] Zhang Q., Xie G., Xu M., Su Y., Tai H., Du H., Jiang Y., *Sensor. Actuat. B-Chem.* **2018**, *259*, 269-281.
[32] Yang Z., Guo L., Zu B., Guo Y., Xu T., Dou X., *Adv. Optical Mater.* **2014**, *2*, 738-745.
[33] Park S., An S., Mun Y., Lee C., *ACS Appl. Mater. Inter.* **2013**, *5*, 4285-4292.
[34] Lu G., Xu J., Sun J., Yu Y., Zhang Y., Liu F., *Sensor. Actuat. B-Chem.* **2012**, *162*, 82-88.
[35] Chen R., Wang J., Xia Y., Xiang L., *Sensor. Actuat. B-Chem.* **2018**, *255*, 2538-2545.
[36] Cui S., Wen Z., Huang X., Chang J., Chen J., *Small* **2015**, *11*, 2305-2313.
[37] Wang J., Li X., Xia Y., Komarneni S., Chen H., Xu J., Xiang L., Xie D., *ACS Appl. Mater. Inter.* **2016**, *8*, 8600-8607.
[38] Gaiardo A., Fabbri B., Giberti A., Guidi V., Bellutti P., Malagu C., Valt M., Pepponi G., Gherardi S., Zonta G., Martucci A., Sturaro M., Landini N., *Sensor. Actuat. B-Chem.* **2016**, *237*, 1085-1094.
[39] Laminack W. I., Gole J. L., *Adv. Funct. Mater.* **2013**, *23*, 5916-5924.
[40] Mane A. T., Navale S. T., Sen S., Aswal D. K., Gupta S. K., Patil V. B., *Org. Electron.* **2015**, *16*, 195-204.
[41] Su P.-G., Peng S.-L., *Talanta.* **2015**, *132*, 398-405.
[42] Mane A. T., Navale S. T., Patil V. B., *Org. Electron.* **2015**, *19*, 15-25.
[43] Nalage S. R., Mane A. T., Pawar R. C., Lee C. S., Patil V. B., *Ionics.* **2014**, *20*, 1607-1616.
[44] Gu F., Nie R., Han D., Wang Z., *Sensor. Actuat. B-Chem.* **2015**, *219*, 94-99.
[45] Xu X., Wang D., Wang W., Sun P., Ma J., Liang X., Sun Y., Ma Y., Lu G., *Sensor. Actuat. B-Chem.* **2012**, *171*, 1066-1072.
[46] Late D. J., Huang Y.-K., Liu B., Acharya J., Shirodkar S. N., Luo J., Yan A., Charles D., Waghmare U. V., Dravid V. P., Rao C. N. R., *ACS Nano* **2013**, *7*, 4879-4891.
[47] Xu T., Pei Y., Liu Y., Wu D., Shi Z., Xu J., Tian Y., Li X., *J. Alloy. Compd.* **2017**, *725*, 253-259.
[48] He Q., Zeng Z., Yin Z., Li H., Wu S., Huang X., Zhang H., *Small* **2012**, *8*, 2994-2999.
[49] Li H.-Y., Yoon J.-W., Lee C.-S., Lim K., Yoon J.-W., Lee J.-H., *Sensor. Actuat. B-Chem.* **2018**, *255*, 2963-2970.
[50] Cha J.-H., Choi S.-J., Yu S., Kim I.-D., *J. Mater. Chem. A.* **2017**, *5*, 8725-8732.
[51] Ko K. Y., Song J.-G., Kim Y., Choi T., Shin S., Lee C. W., Lee K., Koo J., Lee H., Kim J., Lee T., Park J., Kim H., *ACS Nano* **2016**, *10*, 9287-9296.
[52] Liu H., Li M., Voznyy O., Hu L., Fu Q., Zhou D., Xia Z., Sargent E. H., Tang J., *Adv. Mater.* **2014**, *26*, 2718-2724.
[53] Fahad H. M., Shiraki H., Amani M., Zhang C., Hebbar V. S., Gao W., Ota H., Hettick M., Kiriya D., Chen Y.-Z., Chueh Y.-L., Javey A., *Sci. Adv.* **2017**, *3*, 1602557-1602565.
[54] Park H., Jung H., Zhang M., Chang C. H., Ndifor-Angwafor N. G., Choa Y., Myung N. V., *Nanoscale.* **2013**, *5*, 3058-3062.
[55] Cho S.-Y., Lee Y., Koh H.-J., Jung H., Kim J.-S., Yoo H.-W., Kim J., Jung H.-T., *Adv. Mater.* **2016**, *28*, 7020-7029.
[56] Cui S., Pu H., Wells S. A., Wen Z., Mao S., Chang J., Hersam M. C., Chen J., *Nat. Commun.* **2015**, *6*, 8632-8641.
[57] Ghanbari K., *Synthetic Met.* **2014**, *195*, 234-240.
[58] Zhang Y., Kim J. J., Chen D., Tuller H. L., Rutledge G. C., *Adv. Funct. Mater.* **2014**, *24*, 4005-4014.
[59] Jalil A. R., Chang H., Bandari V. K., Robaschik P., Zhang J., Siles P. F., Li G., Buerger D., Grimm D., Liu X., Salvan G., Zahn D. R. T., Zhu F., Wang H., Yan D., Schmidt O. G., *Adv. Mater.* **2016**, *28*, 2971-2977.
[60] Ji S., Wang H., Wang T., Yan D., *Adv. Mater.* **2013**, *25*, 1755-1760.
[61] Zhuang Y., Yuan W., Qian L., Chen S., Shi G., *Phys. Chem. Chem. Phys.* **2017**, *19*, 12876-12881.
[62] Wang B., Zuo X., Wu Y., Chen Z., He C., Duan W., *Sensor. Actuat. B-Chem.* **2011**, *152*, 191-195.
[63] Han D., Yang W., Gu F., Wang Z., *Sensor. Actuat. B-Chem.* **2018**, *255*, 1139-1146.
[64] Navale S. T., Mane A. T., Khuspe G. D., Chougule M. A., Patil V. B., *Synthetic Met.* **2014**, *195*, 228-233.
[65] Jiang H., Cao L., Li Y., Li W., Ye X., Deng W., Jiang X., Wang G., Xu G., *Chem.Commun.* **2020**, *56*, 5366-5369.
[66] Yuan W., Huang L., Zhou Q., Shi G., *ACS Appl. Mater. Inter.* **2014**, *6*, 17003-17008.
[67] Randeniya L. K., Shi H., Barnard A. S., Fang J., Martin P. J., Ostrikov K., *Small* **2013**, *9*, 3993-3999.
[68] Paul R. K., Badhulika S., Saucedo N. M., Mulchandani A., *Anal. Chem.* **2012**, *84*, 8171-8178.
[69] Su P.-G., Shieh H.-C., *Sensor. Actuat. B-Chem.* **2014**, *190*, 865-872.
[70] Tjoa V., Jun W., Dravid V., Mhaisalkar S., Mathews N., *J. Mater. Chem.* **2011**, *21*, 15593-15599.
[71] Chia L. S., Du Y. H., Palale S., Lee P. S., *ACS Omega.* **2019**, *4*, 10388-10395.
[72] Kumar R., Jenjeti R. N., Sampath S., *ACS Sensors.* **2020**, *5*, 404-411.
[73] Cho B., Kim A. R., Park Y., Yoon J., Lee Y.-J., Lee S., Yoo T. J., Kang C. G., Lee B. H., Ko H. C., Kim D.-H., Hahm M. G., *ACS Appl. Mater. Inter.* **2015**, *7*, 2952-2959.
[74] Sharma A., Tomar M., Gupta V., *J. Mater. Chem.* **2012**, *22*, 23608-23616.
[75] Sun Q., Hao J., Zheng S., Wan P., Li J., Zhang D., Li Y., Wang T., Wang Y., *Nanotechnology* **2020**, *31*, 425502-425511.

[76] Liu L., Ikram M., Ma L., Zhang X., Lv H., Ullah M., Khan M., Yu H., Shi K., *J. Hazard. Mater.* **2020**, *393*, 122325-122335.
[77] Abbas A. N., Liu B., Chen L., Ma Y., Cong S., Aroonyadet N., Koepf M., Nilges T., Zhou C., *ACS Nano* **2015**, *9*, 5618-5624.
[78] Sangeetha M., Madhan D., *Opt. Laser Technol.* **2020**, *127*, 106193-106203.
[79] Wang Y., Liu D., Yin J., Shang Y., Du J., Kang Z., Wang R., Chen Y., Sun D., Jiang J., *Chem. Commun.* **2020**, *56*, 703-706.
[80] Niu F., Shao Z.-W., Gao H., Tao L.-M., Ding Y., *Sensor. Actuat. B-Chem.* **2021**, *328*, 129005.
[81] Gomez-Navarro C., Weitz R. T., Bittner A. M., Scolari M., Mews A., Burghard M., Kern K., *Nano Lett.* **2009**, *7*, 3499–3503.
[82] Wu J., Wu Z., Ding H., Yang X., Wei Y., Xiao M., Yang Z., Yang B.-R., Liu C., Lu X., Qiu L., Wang X., *ACS Sensors* **2019**, *4*, 1889-1898.
[83] Jiang W., Chen X., Wang T., Li B., Zeng M., Yang J., Hu N., Su Y., Zhou Z., Yang Z., *Rsc Adv.* **2021**, *11*, 5618-5628.
[84] Jiang W., Wang T., Chen X., Li B., Zeng M., Hu N., Su Y., Zhou Z., Zhang Y., Yang Z., *Phys. Chem. Chem. Phys.* **2020**, *22*, 18499-18506.
[85] Khan M. A. H., Thomson B., Debnath R., Rani A., Motayed A., Rao M. V., *Nanotechnology.* **2020**, *31*, 155504-155515.
[86] Guo J., Wen R., Zhai J., Wang Z. L., *Sci. Bull.* **2019**, *64*, 128-135.
[87] Wang J., Shen Y., Li X., Xia Y., Yang C., *Sensor. Actuat. B-Chem.* **2019**, *298*, 126858-126867.
[88] Zhou Y., Gao C., Guo Y., *J. Mater. Chem. A.* **2018**, *6*, 10286-10296.
[89] Wu T., Wang Z., Tian M., Miao J., Zhang H., Sun J., *Sensor. Actuat. B-Chem.* **2018**, *259*, 526-531.
[90] Giampiccolo A., Tobaldi D. M., Leonardi S. G., Murdoch B. J., Seabra M. P., Ansell M. P., Neri G., Ball R. J., *Appl. Catal., B. Environ.* **2019**, *243*, 183-194.
[91] Liu B., Luo Y., Li K., Wang H., Gao L., Duan G., *Adv. Mater. Interfaces.* **2019**, *6*.
[92] Wang Z., Zhang T., Zhao C., Han T., Fei T., Liu S., Lu G., *J. Colloid Interface Sci.* **2018**, *514*, 599-608.
[93] Liu Y., Gao X., Li F., Lu G., Zhang T., Barsan N., *Sens. Actuators B-Chem.* **2018**, *260*, 927-936.
[94] Wang Z., Men G., Zhang R., Gu F., Han D., *Sens. Actuators, B-Chem.* **2018**, *263*, 218-228.
[95] Wu E., Xie Y., Yuan B., Zhang H., Hu X., Liu J., Zhang D., *ACS Sensors* **2018**, *3*, 1719-1726.
[96] Aziz A., Tiwale N., Hodge S. A., Attwood S. J., Divitini G., Welland M. E., *ACS Appl. Mater. Inter.* **2018**, *10*, 43817-43823.

